

Influence on the conversion of DMS to MSA and SO_4^{2-} in the Southern Ocean, Antarctica

Jinpei Yan ^{a,b,*}, Miming Zhang ^{a,b}, Jinyoung Jung ^c, Qi Lin ^{a,b}, Shuhui Zhao ^{a,b}, Suqing Xu ^{a,b}, Liqi Chen ^{a,b}

^a Key Laboratory of Global Change and Marine-Atmospheric Chemistry, MNR, Xiamen, 361005, China

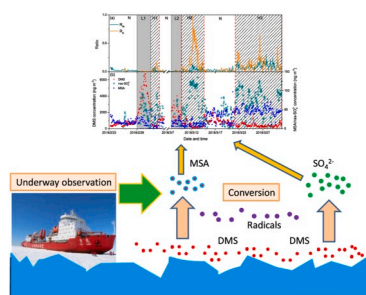
^b Third Institute of Oceanography, Ministry of Natural Resources, Xiamen, 361005, China

^c Korea Polar Research Institute, 26 Songdomirae-ro, Yeosu-gu, Incheon, 21990, Republic of Korea

HIGHLIGHTS

- Air DMS, MSA and SO_4^{2-} were measured with high-time-resolution in the Southern Ocean.
- MSA and SO_4^{2-} concentrations were not associated with air MSA levels.
- The conversion rates of DMS to MSA were very low even in high air DMS levels.
- The DMS level was much higher than its conversion products in the Southern Ocean.

GRAPHICAL ABSTRACT



ARTICLE INFO

Keywords:

Dimethyl sulfide (DMS)
Methane sulfonic acid (MSA)
nss- SO_4^{2-}
Aerosol
Antarctica

ABSTRACT

Dimethyl sulfide (DMS), methanesulphonic acid (MSA) and sulfate (SO_4^{2-}) were measured simultaneously at high-time resolution in the Southern Ocean (SO) during February and March 2018, to characterize the conversion of DMS to MSA and SO_4^{2-} in the marine atmosphere. DMS concentrations ranged up to $\sim 10890.5 \text{ ng m}^{-3}$ (with an average of $899.8 \pm 957.9 \text{ ng m}^{-3}$, representing the standard deviation), which were much higher than the MSA concentrations (with an average of $30.6 \pm 16.8 \text{ ng m}^{-3}$) and SO_4^{2-} concentration ($148.1 \pm 32.5 \text{ ng m}^{-3}$) in the aerosol phase. The spatial distribution of MSA was different from the distribution of DMS. The ratio of MSA to DMS (R_M) ranged up to ~ 0.31 , with an average of 0.044 ± 0.045 . R_M value decreased dramatically as DMS concentration increased, when DMS concentration was below 1000 ng m^{-3} . The effects of temperature and relative humidity (RH) on R_M were mostly negligible, indicating that neither DMS concentration, nor RH and temperature was the key parameter for the conversion of DMS to MSA in the SO. Ratios of nss- SO_4^{2-} to DMS (R_S) were used to estimate the conversion of DMS to SO_4^{2-} . The calculated R_S with mean R_p (the ratio of MSA to nss- SO_4^{2-}) value correlated well with the observed R_S , which provided an useful method to estimate the biogenic SO_4^{2-} from the oxidation of DMS in the marine atmosphere, as biogenic SO_4^{2-} levels can be calculated with R_s and DMS concentrations. The estimated biogenic SO_4^{2-} levels ranged up to 163.8 ng m^{-3} , with an average of $47.1 \pm 30.2 \text{ ng m}^{-3}$ in the SO during the cruise. The results extend the knowledge of the conversion of DMS to MSA and SO_4^{2-} in the marine atmosphere.

* Corresponding author. No.178 Daxue Road, Siming district Xiamen, Third Institute of Oceanography, MNR, 361005, PR China.

E-mail address: jpyan@tio.org.cn (J. Yan).

<https://doi.org/10.1016/j.atmosenv.2020.117611>

Received 21 November 2019; Received in revised form 8 May 2020; Accepted 9 May 2020

Available online 16 May 2020

1352-2310/© 2020 Elsevier Ltd. All rights reserved.

1. Introduction

Methanesulphonic acid (MSA) and non-sea-salt sulfate (nss-SO₄²⁻) derived from the oxidation of dimethyl sulfide (DMS) have an important effect on cloud condensation nuclei (CCN) in the marine boundary layer (MBL). It has been suggested that these biogenic aerosols alter the radiation budget of the earth and affect the climate (Charlson et al., 1987; Lovelock et al., 1972). DMS is the most abundant form of biogenic sulfur derived from the marine phytoplankton (Lovelock et al., 1972; Stefels et al., 2007). Biogenic sulfur emission from the Southern Ocean (SO) contributes approximately ~60% of the global annual DMS emission (Lana et al., 2011). DMS was first detected in the Antarctic coastal waters during the austral fall in 1986 (Berresheim, 1987). After that the spatial and temporal distributions of DMS in the atmosphere and sea water were observed using shipboard and land-based measurements in the SO and Antarctica for the past decades (O'Dowd et al., 1997; Berresheim et al., 1998; Barnes et al., 2006; Read et al., 2008). Sulfur-containing aerosols, such as MSA and nss-SO₄²⁻, have also been routinely measured in the SO and Antarctic coastal areas (Preunkert et al., 2008; Kloster et al., 2006), to assess the potential routes of DMS oxidation in the marine atmosphere (Sorooshian et al., 2007; Wang et al., 2014) and to quantify the contribution of DMS to CCN (Korhonen et al., 2008).

The impact of DMS-oxidation products on the climate has been previously investigated (Korhonen et al., 2008; Park et al., 2017). Observational and modeling studies have try to find out the linkage between DMS and CCN in the MBL in the last decades (Leck and Bigg, 2007; Quinn and Bates, 2011; Abbatt et al., 2019). The oxidation routes of DMS and formation mechanisms of MSA and nss-SO₄²⁻ in the marine atmosphere have been investigated both experimentally and theoretically (Barnes et al., 2006; Read et al., 2008). Previous studies have shown that SO₄²⁻ is more effective at new particle formation (NPF) than MSA, while MSA is more likely to condense onto existing particles (Hayashida et al., 2017). However, MSA may also increase the sulfate-cluster formation rate by up to one order of magnitude, increasing cluster stability (Bork et al., 2014). DMS is oxidized via two main reaction pathways: addition and abstraction reactions (Barnes et al., 2006; Davis et al., 1998). Addition reaction favors to occur at low temperature, comparing with abstraction reaction (Von Glasow and Crutzen, 2004). Numerical model calculations of the oxidation of DMS in the MBL have shown that BrO can strongly increase the importance of the addition branch in the oxidation of DMS even in low BrO mixing ratios. Generally, MSA is assumed to be formed in the abstraction pathway, however, MSA may also be formed in the addition pathway (Von Glasow and Crutzen, 2004). That means the MSA production rate may increase in low temperature. Hence, high ratio of MSA to nss-SO₄²⁻ is present in cold seasons (Bates et al., 1992). But the production of MSA is greatly enhanced by the impact of halogens in summer time (Ayers et al., 1999), resulting in the high ratio of MSA to nss-SO₄²⁻ in high temperature. Previous studies have simulated the potential reaction pathway of the oxidation of DMS. However, it is shown that there is still significant uncertainty about the conversion of DMS to MSA and SO₄²⁻ due to the complicated atmospheric processes and multiple impact factors in field observation.

In field campaigns, filter sampling methods are commonly used to determine MSA and SO₄²⁻ concentrations, resulting in low spatial and temporal resolutions (Jung et al., 2014; Preunkert et al., 2007; Read et al., 2008; Zhang et al., 2015). Hence, it is difficult to characterize the conversion of DMS to MSA and SO₄²⁻ using filter sampling methods, as the oxidation of DMS occurs rapidly (Read et al., 2008; Kloster et al., 2006). The dataset of DMS, MSA and SO₄²⁻ in the SO has been significantly expanded in recent years (Bates et al., 1992; Preunkert et al., 2007; Davis et al., 1998; Read et al., 2008). High resolution measurements of MSA by AMS have been reported in previous studies (Phinney et al., 2006; Zorn et al., 2008; Langley et al., 2010). However, the high-time resolution data for biogenic sulfur compounds are still rare

and the conversion of DMS to MSA and SO₄²⁻ is still short of knowledge.

Here, DMS, and sulfur compounds were measured simultaneously for the first time at high-time resolution (10 min for DMS and 1 h for MSA and SO₄²⁻) in the SO during February to March 2018. This study aimed to characterize the conversion of DMS to MSA and SO₄²⁻ in the marine atmosphere. Furthermore, impact factors on the conversion of DMS to MSA and SO₄²⁻ were also analyzed to better understand the products of MSA and SO₄²⁻ from the oxidation of DMS in the SO.

2. Experimental methods and observation regions

The observation was carried out by R/V “Xuelong” during the 34th Chinese Antarctica Expedition Research Cruise, which covered with a large scale of the SO (40°S to 76°S, 170°E to 110°W). The cruise was conducted from 23 February to 31 March 2018.

Meteorological parameters such as temperature, humidity, wind speeds and wind directions were measured continuously using an automated meteorological station deployed in the R/V “Xuelong”.

2.1. Observation instruments and sampling inlet

An in-situ gas and aerosol composition monitoring system (IGAC, Model S-611, Machine Shop, Fortelice International Co., Ltd., Taiwan; <http://www.machine-shop.com.tw/>), and a DMS measurement system with TOF-MS (SPIMS-3000, Guangzhou Hexin Co., Ltd., China) as a detector were employed on the R/V “Xuelong” to measure the gases and aerosols water-soluble ions and DMS, respectively. The sampling inlet connecting to the monitoring instruments was fixed to a mast at 20 m above the sea surface, locating at the bow of the vessel. A total suspended particulate (TSP) sample inlet was positioned at the top of the mast. Conductive silicone tubing with an inner diameter of 1.0 cm was used to make the connection to all aerosol observation instruments and Teflon tubing with an inner diameter of 0.6 cm was used for DMS measurement.

2.2. Aerosol water soluble ions measurement

For IGAC measurement, gases and aerosols were separated and streamed into a liquid effluent for on-line chemical analysis at an hourly temporal resolution (Young et al., 2016; Liu et al., 2017). The analytical design and methodology for the determination of gases and aerosols water-soluble ions have been described in detail in previous studies (Tao et al., 2018; Yan et al., 2019). Fine particles were firstly enlarged by vapor condensation and subsequently collected on the impaction plate. The samples were then analyzed for anions and cations by an on-line ion chromatography (IC) system (DionexICS-3000). Six to eight concentrations of standard solutions were selected for calibration, depending on the target concentration, in which the R² was above 0.997 (Fig. 1). The detection limits for MSA⁻, SO₄²⁻, Na⁺, and Cl⁻ were 0.09, 0.12, 0.03, and 0.03 μg L⁻¹ (aqueous solution), respectively.

2.3. DMS measurement

The analytical design and methodologies for the measurement of sea water and air DMS have been described in detail by Zhang et al. (2019). A TOF-MS (SPI-3000MS, Guangzhou Hexin Company, China) was used as a detector. Polydimethylsiloxane (PDMS, thickness 0.002 int., Technical Products Inc., USA) membrane was used in the TOF-MS injector. The DMS measurements made by the TOF-MS had excellent repeatability (4.94% for seawater measurements and 4.92% for air measurements, Zhang et al., 2019). The calibration curves for the air standard were highly linear (R² = 0.997). The DMS detection limits, calculated as the value of the blank signal plus three times the standard deviation of the blank signal, were 0.07 nM DMS in seawater and 89 ng m⁻³ DMS in air. These values indicated that this instrument was suitable for the detection of DMS in seawater and air. In this study, we did not discuss

the sea water DMS. DMS represented air DMS in the following sections.

3. Results and discussion

3.1. Spatial distribution of DMS, MSA^- and SO_4^{2-} in the SO

The DMS (Zhang et al., 2019), aerosol water-soluble ion species (MSA^- , SO_4^{2-} and Na^+) were measured in the SO during the cruise. The DMS concentrations ranged up to $\sim 10890.5 \text{ ng m}^{-3}$, with an average of $899.8 \pm 957.9 \text{ ng m}^{-3}$ ($n = 7876$, Fig. 2a), which was larger than DMS levels reported in the Antarctica coastal areas, such as Palmer Station (mean DMS 94 ppt, 261 ng m^{-3}) (Berresheim et al., 1998) and Halley Station (maximum DMS value of 0.418 ppb, 1162.6 ng m^{-3}) (Read et al., 2008). In this study, the uncertainties represent the statistical range of the observations (standard deviation). The highest DMS levels were present in the L1 region, averaging $3954.9 \pm 1495.7 \text{ ng m}^{-3}$ ($n = 1932$), followed by $3090.9 \pm 1230.8 \text{ ng m}^{-3}$ ($n = 234$) in the L2 region. In this study, the maximum DMS concentration was $10890.5 \text{ ng m}^{-3}$ (3.91 ppb), similar to DMS level reported in the Dumont d'Urville Station (maximum DMS of 5.5 ppb) (Preunkert et al., 2007). Variation in DMS levels was associated with wind speed (Fig. 3), indicating that the air-sea DMS fluxes increased with the wind speed in the ocean (Nightingale et al., 2000). The results indicated that high-time resolution DMS data improved the understanding of DMS emissions from the sea surface.

The measured MSA level ranged up to $\sim 97.3 \text{ ng m}^{-3}$, with an average of $30.6 \pm 16.8 \text{ ng m}^{-3}$ ($n = 712$) during the cruise (Fig. 2b). The MSA levels observed in this study were consistent with those reported at Mawson station ($67^\circ 36' \text{ S}$, $62^\circ 53' \text{ E}$) with an average of 20 ng m^{-3}

(Prospero et al., 1991), Halley station ($75^\circ 39' \text{ S}$; with an average of 35.3 ng m^{-3}), and Dumont d'Urville station ($66^\circ 40' \text{ S}$), with an average of 49.0 ng m^{-3} (Minikin et al., 1998). MSA is formed exclusively from the oxidation of DMS (Legrand and Pasteur, 1998), however, the spatial distribution of MSA was different from DMS, as seen in Fig. 2a and b. Extremely high DMS concentrations were observed in the L1 region ($130^\circ - 160^\circ \text{ W}$, $69^\circ - 78^\circ \text{ S}$), but MSA levels in this region were not high. In contrast, high MSA concentrations were present during 15–30 March, but the DMS levels were not expected to be high during this period. The DMS concentrations were much higher than MSA concentrations during the cruise, which were consistent with previous observations that MSA and nss-SO_4^{2-} levels decreased rapidly at the end of austral summer (Prospero et al., 1991; Read et al., 2008). These results implied that the conversion of DMS to MSA and SO_4^{2-} were lower efficiency during this time.

SO_4^{2-} and Na^+ concentrations are also illustrated in Fig. 2. SO_4^{2-} concentrations ranged from 34.1 ng m^{-3} to 273.8 ng m^{-3} , with an average of $148.1 \pm 32.5 \text{ ng m}^{-3}$ ($n = 786$, Fig. 2c), while Na^+ concentrations ranged from 15.6 ng m^{-3} to 4524.6 ng m^{-3} , with an average of 822.4 ± 826.5 ($n = 786$, Fig. 2d). The SO_4^{2-} levels measured here were similar to those measured at Halley Station (mean: 115.0 ng m^{-3}) but lower than those measured at Neumayer Station (mean: 312.0 ng m^{-3}) and Dumont d'Urville Station (mean: 372.0 ng m^{-3}). Unlike MSA^- , SO_4^{2-} is derived from multiple sources, such as sea salt aerosols, anthropogenic emissions, and marine biogenic or volcanic sources (Legrand and Pasteur, 1998; Hayashida et al., 2017). However, in high latitude regions of the SO, SO_4^{2-} was mainly associated with sea salt and biogenic sources (Berresheim et al., 1998). In this study, the temporal

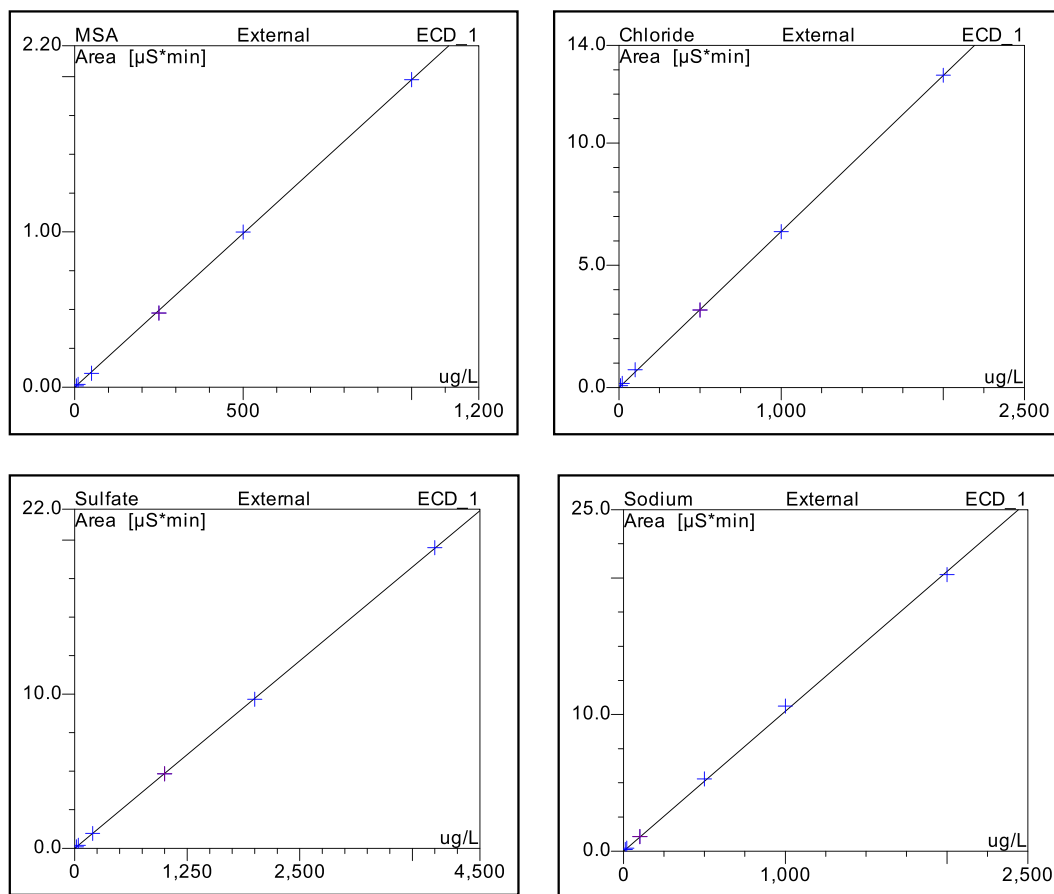


Fig. 1. Calibration curves of MSA, chloride, sulfate and sodium for IGAC monitoring system. (a) Six out of eight concentrations of standard solutions ($0.1\text{--}1000 \text{ }\mu\text{g L}^{-1}$) were selected for MSA calibration ($R^2 = 0.998$), (b) Six out of eight concentrations of standard solutions ($0.1\text{--}2000 \text{ }\mu\text{g L}^{-1}$) were selected for Chloride calibration ($R^2 = 0.997$), (c) Six out of eight concentrations of standard solutions ($0.1\text{--}4000 \text{ }\mu\text{g L}^{-1}$) were selected for Sulfate calibration ($R^2 = 0.997$), (d) Six out of eight concentrations of standard solutions ($0.1\text{--}2000 \text{ }\mu\text{g L}^{-1}$) were selected for Sodium calibration ($R^2 = 0.998$).

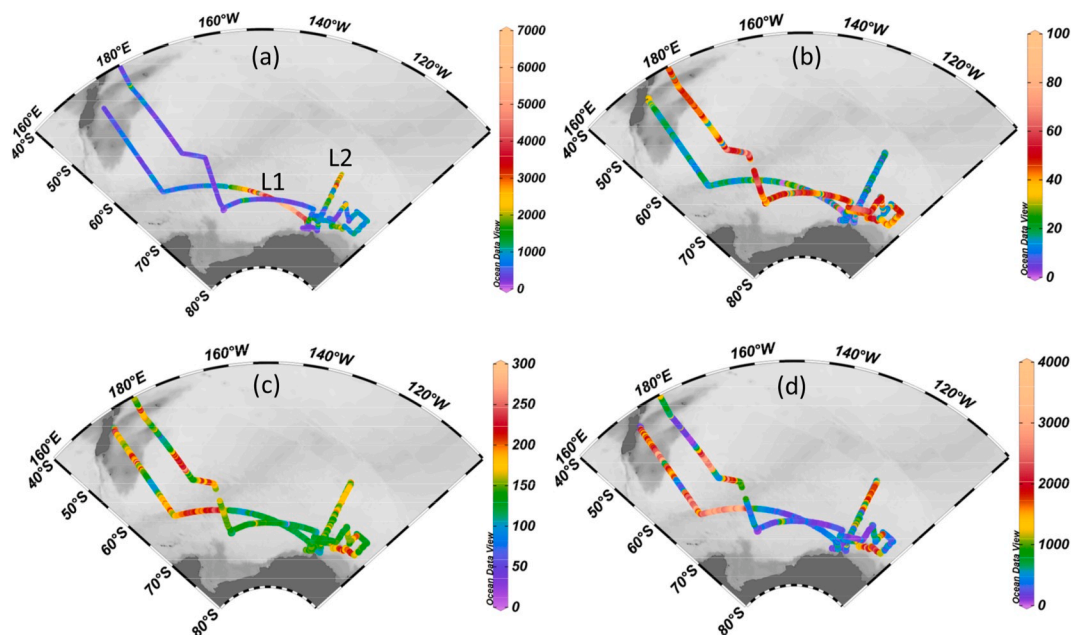


Fig. 2. Spatial distribution of DMS, aerosol MSA^- , SO_4^{2-} and Na^+ in the Amundsen Sea, Antarctica. (a) DMS concentrations ($ng\ m^{-3}$), (b) MSA^- concentrations ($ng\ m^{-3}$), (c) SO_4^{2-} concentrations ($ng\ m^{-3}$), and (d) Na^+ concentrations ($ng\ m^{-3}$).

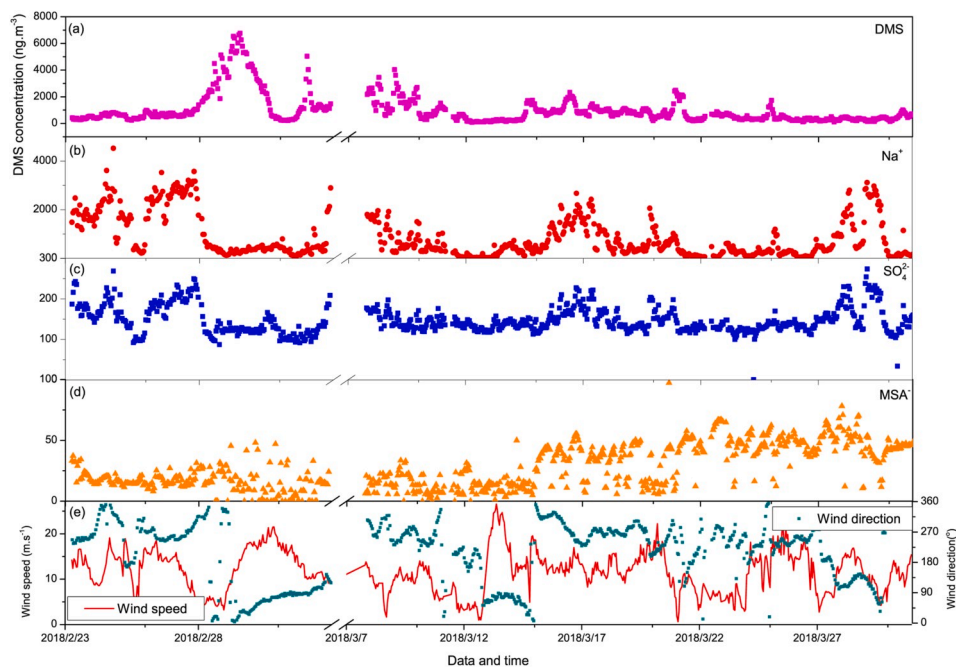


Fig. 3. Temporal distributions of DMS and aerosol compounds. (a) Time series of DMS, (b) Time series of Na^+ , (c) Time series of SO_4^{2-} , (d) Time series of MSA^- , (e) Time series of wind speeds and directions.

distribution of SO_4^{2-} differed noticeably from that of MSA^- (Fig. 3), but high SO_4^{2-} concentration occurred at high Na^+ concentration regions in this study (Fig. 2c and d). Generally, Na^+ is considered to be a marker of sea salt particles in the marine atmosphere (Yan et al., 2018; Legrand and Pasteur, 1998), indicating that SO_4^{2-} in this study was highly impacted by sea salt aerosols, especially where high level of sea spray aerosols occurred. Similar distributions in Na^+ levels and wind speeds were also present (Fig. 3), implying that Na^+ was derived from the sea spray aerosols.

3.2. Conversion of DMS to MSA^- and SO_4^{2-}

MSA^- and SO_4^{2-} are the main products from the oxidation of DMS (Barnes et al., 2006; Read et al., 2008). However, the distributions of MSA^- and SO_4^{2-} differed from those of DMS, Fig. 3. Temporal variations in the ratios of DMS to MSA^- and SO_4^{2-} is given in Fig. 4a. R_M and R_S is defined as the molar ratios of MSA^- to DMS and the molar ratios of $nss-SO_4^{2-}$ to DMS, respectively. $nss-SO_4^{2-}$ concentrations were calculated as follow:

$$[nss - SO_4^{2-}] = [SO_4^{2-}]_{total} - K[Na^+]$$

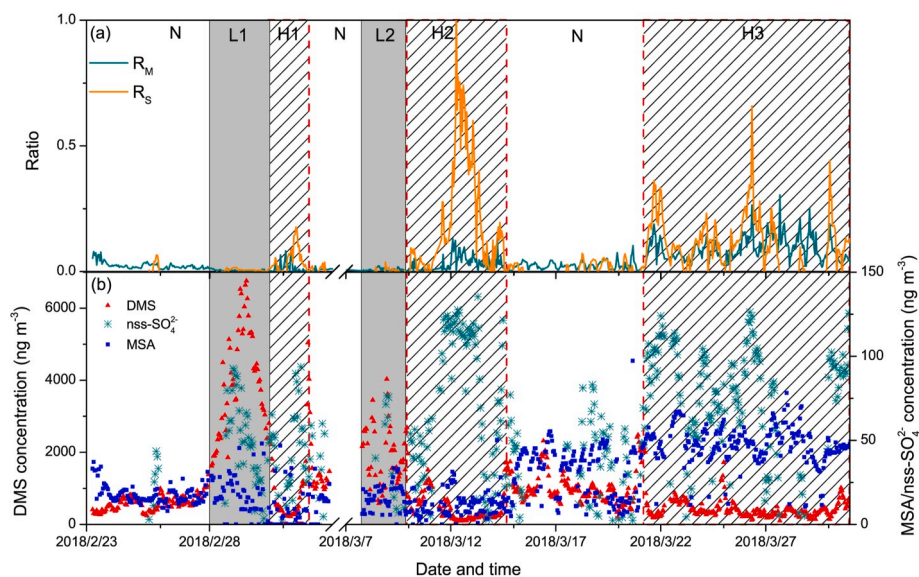


Fig. 4. Temporal distributions of R_S and R_M and sulfur-containing compounds. (a) Time series of R_S and R_M , (b) Time series of DMS, MSA and nss-SO_4^{2-} concentrations.

Where, K equals 0.252, the weight ratio of sulfate and sodium in seawater (Millero and Sohn, 1992).

High R_M and R_S values occurred in H1, H2 and H3 regions (with mean R_M value exceeds 0.03 and mean R_S value exceeds 0.08, seen in Fig. 4) during the cruise. Generally, less DMS may decrease the subsequent production of MSA and nss-SO_4^{2-} , leading to lower R_M and R_S . R_S level was similar to R_M in H1 (mean: 0.08 ± 0.05 and 0.03 ± 0.03 , respectively) and H3 region (mean: 0.14 ± 0.09 and 0.09 ± 0.05 , respectively). However, R_S (0.24 ± 0.23 ; $n = 89$) was much higher than R_M (0.03 ± 0.03 ; $n = 96$) in the H2 region, seen in Table 1. A greater value of R_S than R_M indicated an oxidation favored formation of SO_4^{2-} compared with MSA (Chen et al., 2018). High DMS concentrations were observed in L1 and L2, while the R_S and R_M values were extremely low in L1 and L2 (with mean R_M value below 0.008 and mean R_S value below 0.01). MSA and nss-SO_4^{2-} levels were much smaller than DMS concentrations (Table 1). The observation results suggest that the conversion of DMS to MSA and SO_4^{2-} were not determined by the DMS concentration, as DMS was sufficient in the marine atmosphere.

Different from the MSA, negative nss-SO_4^{2-} value was present in several regions in this study (Fig. 4b). The reason for negative values has been discussed in previous studies (Hall and Wolff, 1998; Wagenbach et al., 1998), particularly regarding the fractionation of sulfate in aerosols by forming $\text{Na}_2\text{SO}_4 \cdot 10 \text{H}_2\text{O}$ at low temperature. Negative R_S value was present (Fig. 4a), when nss-SO_4^{2-} value was negative. In this case, R_S could not well represent the practical conversion of DMS to SO_4^{2-} in the atmosphere. But R_M value can be used to assess the conversion of DMS to MSA in the marine atmosphere, as MSA was exclusively from the oxidation of DMS. Therefore, R_M was used in this study to

clarify the factors that affected DMS conversion in the atmosphere.

3.3. Effects of DMS on the ratio of MSA to DMS

Potential oxidation reactions of DMS to form MSA with different radicals, such as OH, NO_3 , BrO, and ClO, have been confirmed in the previous studies (Barnes et al., 2006). If DMS level is very high that there might not be enough oxidants, leading to low ratios of MSA to DMS. The value of R_M ranged up to ~ 0.31 , with an average of 0.044 ± 0.045 ($n = 712$) (Fig. 5a). R_M decreased dramatically as DMS concentration increased, when the DMS levels were less than 500 ng m^{-3} . However, the R_M value revealed little change as the increasing DMS, when DMS concentrations exceeded 1000 ng m^{-3} . DMS concentrations had two distinct effects on R_M . First, high levels of DMS may result in the formation of more MSA, possibly increasing R_M . The other one, if MSA production was not determined by DMS, then increased DMS levels would result in a decrease in R_M . Here, we found that MSA concentrations were almost independent of DMS concentrations for DMS greater than about 2000 ng m^{-3} (Fig. 4b). For DMS below about 1000 ng m^{-3} , R_M increased sharply with decreasing DMS levels. When DMS concentrations were much greater than MSA levels, variation of MSA concentrations had little effect on R_M . The relationship between R_M and DMS concentrations can be described by the following equation $y = (39.72 \pm 9.55) * x^{-1.15 \pm 0.04}$ in this study (Fig. 5a).

Favoring the formation of MSA at low temperature has been reported in previous studies (Sievering et al., 2004; Bates et al., 1992). Hence, temperature also has an important effect on R_M . A negative relationship between R_M and temperature is not present in the complete dataset, but it is more evident when the data are classified by the distinct regions (Fig. 5b). A negative correlation between R_M and temperature was present in H1, H2 and H3 regions, corroborating the impact of temperature on MSA formation. However, the decrease in R_M as temperature increasing was tiny, with a maximum slope of 0.0087. This suggests that temperature had a minimal effect on the conversion of DMS to MSA in these regions of SO. Previous studies have shown that high RH values were beneficial to the formation of MSA, as DMS oxidation often occurs with aqueous reactions in the atmosphere (Hoffmann et al., 2016; Read et al., 2008). However, we did not observe an obvious correlation between R_M and RH, even when treating our data as distinct regions (Fig. 5c). It indicated that RH was also not the key parameter affecting the conversion of DMS to MSA in this study.

Table 1

Mean value of DMS, MSA, nss-SO_4^{2-} , R_S and R_M in different regions.

| Regions | L1 | L2 | H1 | H2 | H3 |
|--|---------------------|--------------------|-------------------|-------------------|-------------------|
| R_S | 0.007 ± 0.007 | 0.009 ± 0.03 | 0.08 ± 0.05 | 0.24 ± 0.23 | 0.14 ± 0.09 |
| R_M | 0.005 ± 0.005 | 0.008 ± 0.007 | 0.03 ± 0.03 | 0.03 ± 0.03 | 0.09 ± 0.05 |
| DMS(ng m^{-3}) | 3235.9 ± 1767.1 | 1914.1 ± 794.6 | 343.1 ± 109.3 | 396.7 ± 321.9 | 430.6 ± 268.8 |
| MSA(ng m^{-3}) | 24.8 ± 13.5 | 23.5 ± 8.5 | 15.8 ± 5.2 | 18.2 ± 14.8 | 59.4 ± 20.6 |
| Nss- SO_4^{2-} (ng m^{-3}) | 35.1 ± 19.2 | 26.7 ± 36.9 | 45.9 ± 8.5 | 147.4 ± 114.6 | 93.3 ± 37.5 |

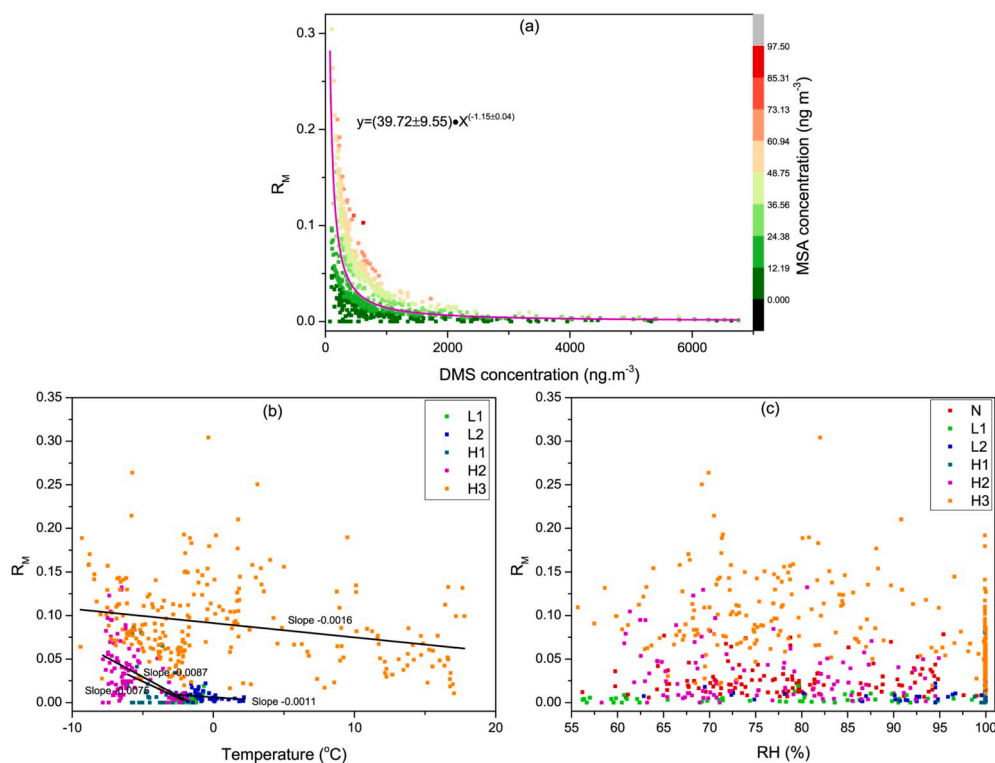


Fig. 5. Impact factors on the ratio of MSA to DMS. (a) Correlation between R_M and DMS concentrations, (b) Correlation between R_M and temperature, (c) Relationship between R_M and relative humidity.

Radical concentrations were not determined in this study. However, previous measurements have found average concentrations of OH and BrO radicals are 0.015 ± 0.009 ppt and 2.7 ± 2.2 ppt, respectively, in the Antarctica boundary layer in February (Read et al., 2008). The oxidant concentrations during this period were similar to MSA levels, consistent with the supposition that the conversion of DMS to MSA and SO_4^{2-} was determined by oxidant levels during late summer in the SO. However, further studies of the impact of radical levels on DMS conversion are required to clarify the parameters affecting the conversion of DMS to MSA and SO_4^{2-} .

3.4. Estimation of the conversion of DMS to SO_4^{2-} in the marine atmosphere

SO_4^{2-} is the other product from the oxidation of DMS in the atmosphere. Nss-SO_4^{2-} is often used to eliminate the effect of sea salt sulfate in the marine atmosphere. But nss-SO_4^{2-} may also consist of anthropogenic and biogenic sulfate in the marine atmosphere (Legrand and Pasteur, 1998). It is very difficult to distinguish biogenic sulfate from anthropogenic sulfate. Sulfur isotope apportionment is useful to identify anthropogenic and biogenic sulfate (Ghahremaninezhad et al., 2016; Li et al., 2018), but the sulfur isotope apportionment was limited for the onboard observation. Generally, the ratio of MSA to nss-SO_4^{2-} (R_p) provides important insight into the oxidation routes of DMS (De Baar et al., 1995; Tortell et al., 2011) and the contribution of different products from the oxidation of DMS. Nss-SO_4^{2-} is mainly derived from marine biogenic sources in high-latitude oceanic regions. The ratio of MSA to nss-SO_4^{2-} can be used to assess marine biogenic production at high latitudes (Saltzman et al., 2006). The ratios of MSA to nss-SO_4^{2-} in the Antarctic coastal and SO have been reported in the previous studies, seen in Table 2. The mean ratios of MSA to nss-SO_4^{2-} concentrated on 0.18 to 0.78 in the Antarctic coastal regions and Southern Ocean during the summer season (Table 2), which is consistent with the observation value in this study. The ratios of MSA to nss-SO_4^{2-} ranged from 0.2 to 0.8, with an average of 0.64 ± 0.59 in this study (Fig. 6a).

As mentioned above, negative nss-SO_4^{2-} values were observed in some regions during the cruise (Fig. 4b). In this case, the observed nss-SO_4^{2-} to DMS ratios (R_S) were also negative (Fig. 6b). It was difficult to assess the R_S when nss-SO_4^{2-} was negative. But R_S can be calculated by the following equation $R_S = R_M/R_p$. The calculated R_S lines with different R_p ($R_{p \text{ Min}} = 0.18$, $R_{p \text{ Mean}} = 0.64$, $R_{p \text{ Max}} = 0.78$) value are illustrated in Fig. 6b. The calculated R_S value using $R_{p \text{ Min}}$ value was much greater than R_S values calculated using $R_{p \text{ Mean}}$, while the calculated R_S with $R_{p \text{ Max}}$ was smaller than R_S values calculated using $R_{p \text{ Mean}}$. R_S value calculated based on $R_{p \text{ Mean}}$ ranged up to ~ 0.51 , with an average of 0.073, consisting with the observed R_S during the cruise, except in the H2 region (Fig. 6b). The observed R_S value was significantly greater than the calculated R_S value in the H2 region. Extremely high concentrations of nss-SO_4^{2-} were observed in this region, however, we did not observe high levels of MSA in this region. It indicated that other sources, in addition to biogenic sources, contributed significantly to nss-SO_4^{2-} in this region. Thus, the R_S value did not reflect the practical conversion of DMS to SO_4^{2-} . The variation of calculated R_S with mean $R_{p \text{ Mean}}$ was consistent well with observed R_S during the observation periods (Fig. 6b). This suggested that calculated R_S based on $R_{p \text{ Mean}}$ could be used to characterize the SO_4^{2-} from the oxidation of DMS in the Southern Ocean, especially when nss-SO_4^{2-} value was negative or influenced by other sources in the marine atmosphere.

It is difficult to assess the biogenic SO_4^{2-} , when nss-SO_4^{2-} is affected by anthropogenic sources or negative nss-SO_4^{2-} value occurred. However, concentrations of biogenic nss-SO_4^{2-} could be achieved using the calculated R_S . The calculated nss-SO_4^{2-} levels with $R_{p \text{ Min}}$ were much greater than the observed nss-SO_4^{2-} concentrations. While the calculated nss-SO_4^{2-} levels based on calculated mean R_S were generally highly consistent with the concentrations of observed nss-SO_4^{2-} during the cruise, except in the H2 region. The observed nss-SO_4^{2-} concentrations were much higher than the calculated nss-SO_4^{2-} concentrations in the H2 region (Fig. 6c). Hence, the calculated nss-SO_4^{2-} using the calculated mean R_S enables us to estimate the biogenic SO_4^{2-} over the SO atmosphere, as biogenic SO_4^{2-} levels can be calculated with R_S and DMS concentrations. The estimated

Table 2
Mean value of MSA to nss-SO₄²⁻ ratio observed in the Antarctic.

| Observation site | Observation time | Mean ratio of MSA to nss-SO ₄ ²⁻ (R _p) | References |
|---------------------|------------------|--|----------------------------|
| Southern Hemisphere | Jan. | 0.23 | Ayers et al. (1997) |
| Southern Hemisphere | Jul. | 0.09 | Ayers et al. (1997) |
| Antarctic | Mar.–Apr. | 0.78 | Berresheim (1987) |
| Antarctic | Mar.–Apr. | 0.54 | Pszenny et al. (1989) |
| Southern Hemisphere | Feb.–Mar. | 0.32 | Bates et al. (1992) |
| Southern Ocean | Dec.–Mar. | 0.18–0.21 | Xu et al. (2013) |
| Mawson, Antarctica | Feb. | 0.31 | Prospero et al. (1991) |
| Southern Hemisphere | Jan.–Feb. | 0.31–0.32 | Arimoto et al. (2001) |
| Antarctica | Jan.–Feb. | 0.65 ± 0.13 | Read et al. (2008) |
| Halley station | Jan. | 0.49 ± 0.05 | Legrand and Pasteur (1998) |
| Neumeyer | Jan. | 0.46 ± 0.17 | Legrand and Pasteur (1998) |
| Dumont d'Urville | Mar. | 0.28 ± 0.05 | Legrand and Pasteur (1998) |
| Southern Ocean | Dec.–Mar. | 0.23 | Chen et al. (2012) |
| Antarctic | Jan.–Feb. | 0.32 | Savoie et al. (1992) |
| Southern Ocean | Summer season | 0.41 | Berresheim et al. (1990) |
| Palmer station | Summer season | 0.61 | Berresheim et al. (1998) |
| Palmer station | Summer season | 0.58 | Savoie et al. (1993) |
| Coastal Antarctic | Dec.–Mar. | 0.3–0.45 | Legrand and Pasteur (1998) |
| Mawson, Antarctica | May.–Sept. | 0.17 | Minikin et al. (1998) |
| Dumont d'Urville | May.–Sept. | 0.31 | Minikin et al. (1998) |
| Southern Ocean | Dec.–Jan. | 0.33 | Yan et al. (2019) |
| Southern Ocean | Feb.–Mar. | 0.64 | This study |

biogenic SO₄²⁻ levels ranged up to 163.8 ng m⁻³, with an average of 47.1 ± 30.2 ng m⁻³ in the SO during the cruise.

4. Conclusions

The conversion of the DMS to MSA and SO₄²⁻ is important for biogenic sulfur cycles and climate change. DMS, gaseous and aerosol sulfur compounds were determined simultaneously for the first time with high-time resolution (10 min for DMS and 1 h for MSA and SO₄²⁻) in the SO to access the conversion of DMS to MSA and SO₄²⁻ and their impact factors. High DMS concentrations were observed with an average of 899.8 ± 957.9 ng m⁻³ (n = 7876), which were much greater than the MSA and SO₄²⁻ concentrations. The ratio of MSA to DMS (R_M) ranged up to ~0.31 (mean: 0.044 ± 0.045), indicating that DMS was sufficient for the conversion of DMS to MSA. Ratios of nss-SO₄²⁻ to DMS (R_S) were calculated to analyze the conversion of DMS to SO₄²⁻. The calculated R_S with mean R_p (the ratio of MSA to nss-SO₄²⁻) value correlated well with the observed R_S, which is useful to understand the conversion of DMS to SO₄²⁻. The calculated nss-SO₄²⁻ levels (ranged up to 163.8 ng m⁻³, with an average of 47.1 ± 30.2 ng m⁻³) based on calculated mean R_S were generally consistent with the concentrations of observed nss-SO₄²⁻ (with an average of 69.4 ± 35.4 ng m⁻³) during the cruise.

R_M value decreased dramatically as DMS concentrations increased, when DMS levels were below 500 ng m⁻³. However, the R_M value revealed little change as the increasing DMS, when DMS concentrations exceeded 1000 ng m⁻³. No obvious correlation between R_M and RH was observed, even when the data was grouped by region. Thus, neither DMS concentration, nor RH, nor temperature were key in controlling the conversion of DMS to MSA in the SO. It was hypothesized that the conversion of DMS to MSA and SO₄²⁻ was governed by the radical levels in the SO during the late summer. However, as radical concentrations were not determined in this study, the impact of radicals on the conversion of DMS to the MSA and SO₄²⁻ remains uncertain. Further studies of the conversion of DMS to MSA and SO₄²⁻ in the marine atmosphere and factors affecting this conversion are required to better understand the behavior of DMS and the formation of MSA and SO₄²⁻ in the SO.

Declaration of competing interest

The authors declare that they have no known competing financial

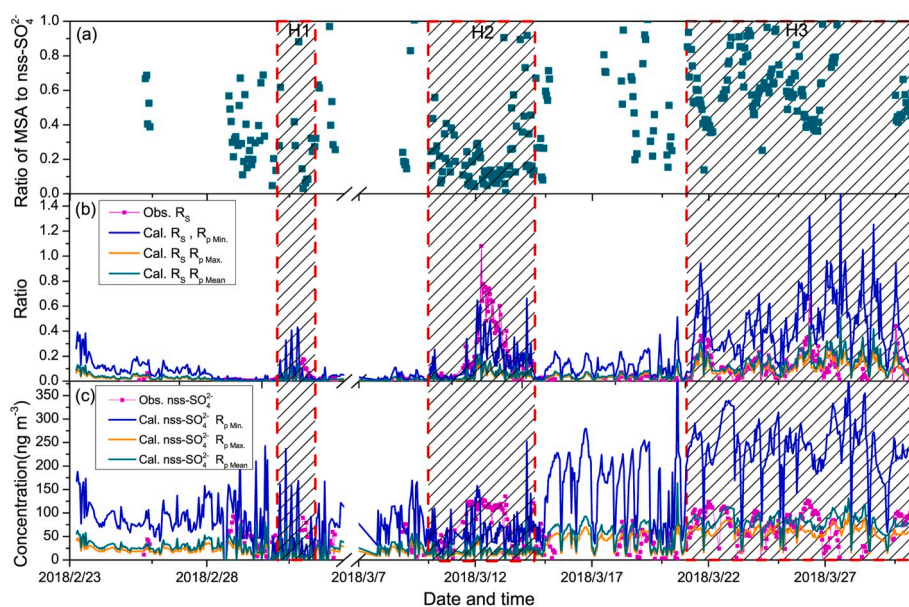


Fig. 6. Calculated R_s and biogenic nss-SO₄²⁻. (a) Ratios of MSA to nss-SO₄²⁻ from observations, (b) Time series of observed R_s and calculated R_s, (c) Time series of observed nss-SO₄²⁻ and calculated nss-SO₄²⁻.

interests or personal relationships that could have appeared to influence the work reported in this paper.

CRedit authorship contribution statement

Jinpei Yan: Conceptualization, Writing - original draft, Data curation, Visualization, Supervision, Project administration, Funding acquisition. **Miming Zhang:** Investigation, Resources, Data curation, Validation. **Jinyoung Jung:** Writing - review & editing, Funding acquisition. **Qi Lin:** Formal analysis, Data curation. **Shuhui Zhao:** Resources. **Suqing Xu:** Data curation. **Liqi Chen:** Writing - review & editing.

Acknowledgements

This study is Financially Supported by Qingdao National Laboratory for marine science and technology (No. QNLM2016ORP0109), the Natural Science Foundation of Fujian Province, China (No. 2019J01120), the National Natural Science Foundation of China (No. 41941014), the response and feedback of the Southern Ocean to climate change (RFSOCC2020-2025), the Chinese Projects for Investigations and Assessments of the Arctic and Antarctic (CHINARE2017-2020). Jinyoung Jung was supported by grants from Korea Polar Research Institute (KOPRI) (No. PE20140). The authors gratefully acknowledge Guangzhou Hexin Analytical Instrument Co., Ltd., for the on-board observation technical assistance, and Machine Shop, Fortelice International Co., Ltd., for the IGAC technical assistance and data analysis.

Appendix A. Supplementary data

Supplementary data to this article can be found online at <https://doi.org/10.1016/j.atmosenv.2020.117611>.

References

- Abbatt, J.P.D., Leaitch, W.R., Aliabadi, A.A., Bertram, A.K., Blanchet, J.P., Boivin-Rioux, A., Bozem, H., Burkart, J., Chang, R.Y.W., Charette, J., Chaubey, J.P., Christensen, R.J., Cirisan, A., Collins, D.B., Croft, B., Dionne, J., Evans, G.J., Fletcher, C.G., Gali, M., Ghahremaninezhad, R., Girard, E., Gong, W., Gosselin, M., Gourdal, M., Hanna, S.J., Hayashida, H., Herber, A.B., Hesarki, S., Hoor, P., Huang, L., Husserr, R., Irish, V.E., Keita, S.A., Kodros, J.K., Köllner, F., Kolonjari, F., Kunkel, D., Ladino, L.A., Law, K., Lévassieur, M., Libois, Q., Liggio, J., Lizotte, M., Macdonald, K.M., Mahmood, R., Martin, R.V., Mason, R.H., Miller, L.A., Moravek, A., Mortenson, E., Mungal, E.L., Murphy, J.G., Namazi, M., Norman, A., O'Neill, N.T., Pierce, J.R., Russell, L.M., Schneider, J., Schulz, H., Sharma, S., Si, M., Staebler, R.M., Steiner, N.S., Thomas, J.L., Salzen, K., Wentzell, J.B., Willis, M.D., Wentworth, G.R., Xu, J.W., Yakobi-Hancock, J.D., 2019. Overview paper: insights into aerosol and climate in the Arctic. *Atmos. Chem. Phys.* 19, 2527–2560.
- Arimoto, R., Nottingham, A.S., Webb, J., Schloesslin, C.A., Davis, D.D., 2001. Non-sea salt sulfate and other aerosol constituents at the South Pole during ISCAT. *Geophys. Res. Lett.* 28, 3645–3648.
- Ayers, G.P., Cainey, J.M., Gillett, R.W., Ivey, J.P., 1997. Atmospheric sulphur and cloud condensation nuclei in marine air in the Southern Hemisphere. *Phil. Trans. Roy. Soc. Lond.* 352, 203–211.
- Ayers, G.P., Gillett, R.W., Cainey, J.M., Dick, A.L., 1999. Chloride and bromide loss from sea-salt particles in Southern Ocean air. *J. Atmos. Chem.* 33, 299–319.
- Barnes, I., Hjorth, J., Mihalopoulos, N., 2006. Dimethyl sulfide and dimethyl and their oxidation in the atmosphere. *Chem. Rev.* 106, 940–975.
- Bates, T.S., Calhoun, J.A., Quinn, P.K., 1992. Variations in the methane sulphonate to sulphate molar ratio in submicrometer marine aerosol particles over the South Pacific Ocean. *J. Geophys. Res.* 97, 9859–9865.
- Berresheim, H., Huey, J.M., Thorn, R.P., Eisele, F.L., Tanner, D.J., Jefferson, A., 1998. Measurements of dimethyl sulfide, dimethyl sulfoxide, dimethyl sulfone, and aerosol ions at Palmer Station, Antarctica. *J. Geophys. Res.* 103, 1629–1637.
- Berresheim, H., Andreae, M.O., Ayers, G.P., Gillett, R.W., Merrill, J.T., Davis, V.J., Chameides, W.L., 1990. Airborne measurements of dimethylsulfides, sulfur dioxide, and aerosol ions over the southern ocean south of Australia. *J. Atmos. Chem.* 10, 341–370.
- Berresheim, H., 1987. Biogenic sulfur emissions from the subantarctic and antarctic oceans. *J. Geophys. Res.* 92 (D11), 13245–13213.
- Bork, N., Elm, J., Olenius, T., Vehkamäki, H., 2014. Methane sulfonic acid-enhanced formation of molecular clusters of sulfuric acid and dimethyl amine. *Atmos. Chem. Phys.* 14, 12023–12030.
- Charlson, R.J., Lovelock, J.E., Andreae, M.O., Warren, S.G., 1987. Oceanic phytoplankton, atmospheric sulphur, cloud albedo, and climate. *Nature* 326, 655–661.
- Chen, Q., Sherwen, T., Evans, M., Alexander, B., 2018. DMS oxidation and sulfur aerosol formation in the marine troposphere: a focus on reactive halogen and multiphase chemistry. *Atmos. Chem. Phys.* 18, 13617–13637.
- Chen, L., Wang, J., Gao, Y., Xu, G., Yang, X., Lin, Q., Zhang, Y., 2012. Latitudinal distributions of atmospheric MSA and MSA/nss-SO₄²⁻ ratios in summer over the high latitude regions of the Southern and Northern Hemispheres. *J. Geophys. Res.* 117, D10306.
- Davis, D., Chen, G., Kasibhatla, P., Jefferson, A., Tanner, D., Eisele, F., Lenschow, D., Neff, W., Berresheim, H., 1998. DMS oxidation in the Antarctic marine boundary layer: comparison of model simulations and field observations of DMS, DMSO, DMSO₂, H₂SO₄(g), MSA(g), and MSA(p). *J. Geophys. Res.* 103, 1657–1678.
- De Baar, H.J., De Jong, J.T., Bakker, D.C., Löscher, B.M., Veth, C., Bathmann, U., Smetacek, V., 1995. Importance of iron for plankton blooms and carbon dioxide drawdown in the Southern Ocean. *Nature* 373, 412–415.
- Ghahremaninezhad, R., Norman, A.-L., Abbatt, J.P.D., Lévassieur, M., Thomas, J.L., 2016. Biogenic, anthropogenic and sea salt sulfate size-segregated aerosols in the Arctic summer. *Atmos. Chem. Phys.* 16, 5191–5202.
- Hall, J.S., Wolff, E.W., 1998. Causes of seasonal and daily variations in aerosol sea-salt concentrations at a coastal Antarctic station. *Atmos. Environ.* 32, 3669–3677.
- Hayashida, H., Steiner, N., Monahan, A., Galindo, V., Lizotte, M., Lévassieur, M., 2017. Implications of sea-ice biogeochemistry for oceanic production and emissions of dimethyl sulfide in the Arctic. *Biogeosciences* 14, 3129–3155.
- Hoffmann, E.H., Tilgner, A., Schrödner, R., Bräuer, P., Wolk, R., Herrmann, H., 2016. An advanced modeling study on the impacts and atmospheric implications of multiphase dimethyl sulfide chemistry. *Proc. Natl. Acad. Sci. Unit. States Am.* <https://doi.org/10.1073/pnas.1606320113>.
- Jung, J., Furutani, H., Uematsu, M., Park, J., 2014. Distributions of atmospheric non-sea-salt sulfate and methanesulfonic acid over the Pacific Ocean between 48°N and 55°S during summer. *Atmos. Environ.* 99, 374–384.
- Kloster, S., Feichter, J., Maier-Reimer, E., Six, K.D., Stier, P., Wetzell, P., 2006. DMS cycle in the marine ocean-atmosphere system? a global model study. *Biogeosciences* 3, 29–51.
- Korhonen, H., Carslaw, K.S., Spracklen, D.V., Mann, G.W., Woodhouse, M.T., 2008. Influence of oceanic dimethyl sulfide emissions on cloud condensation nuclei concentrations and seasonality over the remote Southern Hemisphere oceans: a global model study. *J. Geophys. Res.* 113, D15204.
- Lana, A., Bell, T.G., Simo, R., Vallina, S.M., Ballabrera-Poy, J., Kettle, A.J., Dachs, J., Bopp, L., Saltzman, E.S., Stefels, J., Johnson, J.E., Liss, P.S., 2011. An updated climatology of surface dimethylsulfide concentrations and emission fluxes in the global ocean. *Global Biogeochem. Cycles* 25, GB1004.
- Langley, L., Leaitch, W.R., Lohmann, U., Shantz, N.C., Worsnop, D.R., 2010. Contributions from DMS and ship emissions to CCN observed over the summertime North Pacific. *Atmos. Chem. Phys.* 10, 1287–1314.
- Leck, C., Bigg, K., 2007. A modified aerosol-cloud-climate feedback hypothesis. *Environ. Chem.* 4, 400–403.
- Legrand, M., Pasteur, E.C., 1998. Methane sulfonic acid to non-sea-salt sulfate ratio in coastal Antarctic aerosol and surface snow. *J. Geophys. Res.* 103, 10991–11006.
- Li, J., Michalski, G., Davy, P., Harvey, M., Katzman, T., Wilkins, B., 2018. Investigating source contributions of size-aggregated aerosols collected in Southern Ocean and baring head, New Zealand using sulfur isotopes. *Geophys. Res. Lett.* 45, 3717–3727.
- Liu, M., Song, Y., Zhou, T., Xu, Z., Yan, C., Zheng, M., Wu, Z., Hu, M., Wu, Y., Zhu, T., 2017. Fine particle pH during severe haze episodes in northern China. *Geophys. Res. Lett.* 44, 5213–5221.
- Lovelock, J.E., Maggs, R.J., Rasmussen, R.A., 1972. Atmospheric dimethyl sulphide and the natural sulphur cycle. *Nature* 237, 452–453.
- Millero, F.J., Sohn, M.L., 1992. *Chemical Oceanography*, vol. 531. CRC Press, Boca Raton, Fla.
- Minikin, A., Legrand, M., Hall, J., Wagenbach, D., Kleefeld, C., Wolff, E., Pasteur, E.C., Ducroz, F., 1998. Sulfur-containing species (sulfate and methanesulfonate) in coastal Antarctic aerosol and precipitation. *J. Geophys. Res.* 103, 10975–10990.
- Nightingale, P.D., Malin, G., Law, C.S., Watson, A.J., Liss, P.S., Liddicoat, M.I., Boutin, J., Upstill-Goddard, R.C., 2000. In situ evaluation of air-sea gas exchange parameterizations using novel conservative and volatile tracers. *Global Biogeochem. Cycles* 14, 373–387.
- O'Dowd, C.D., Lowe, J.A., Smith, M.H., Davison, B., Hewitt, C.N., Harrison, R.M., 1997. Biogenic sulphur emissions and inferred non-sea salt sulphate cloud condensation nuclei in and around Antarctica. *J. Geophys. Res.* 102, 12839–12854.
- Park, K., Jang, S., Lee, K., Yoon, Y.J., Kim, M., Park, K., Cho, H., Kang, J., Udisti, R., Lee, B., Shin, K., 2017. Observational evidence for the formation of DMS-derived aerosols during Arctic phytoplankton bloom. *Atmos. Chem. Phys.* 17, 9665–9675.
- Phinney, L., Leaitch, W.R., Lohmann, U., Boudries, H., Toom-Saunty, D., Sharma, S., Shantz, N., 2006. Characterization of aerosol over the sub-arctic NE pacific during SERIES. *Deep-Sea Res. II* 53, 2410–2433.
- Preunkert, S., Jourdain, B., Legrand, M., Udisti, R., Becagli, S., Cerri, O., 2008. Seasonality of sulfur species (dimethyl sulfide, sulfate, and methanesulfonate) in Antarctica: Inland versus coastal regions. *J. Geophys. Res.* 113 (D15302).
- Preunkert, S., Legrand, M., Jourdain, B., Moulin, C., Belviso, S., Kasamatsu, N., Fukuchi, M., Hirawake, T., 2007. Interannual variability of dimethylsulfide in air and seawater and its atmospheric oxidation by-products (methanesulfonate and sulphate) at Dumont d'Urville, coastal Antarctica (1999–2003). *J. Geophys. Res.* 112.
- Prospero, J.M., Savoie, D.L., Saltzman, E.S., Larsen, R., 1991. Impact of oceanic sources of biogenic sulphur on sulphate aerosol concentrations at Mawson, Antarctica. *Nature* 350, 221–223.

- Pszenny, A.P., Castelle, A.J., Galloway, J.N., 1989. A study of the sulfur cycle in the Antarctic marine boundary layer. *J. Geophys. Res.* 94, 9818–9830.
- Quinn, P.K., Bates, T.S., 2011. The case against climate regulation via oceanic phytoplankton sulphur emissions. *Nature* 480, 51–56.
- Read, K.A., Lewis, A.C., Bauguitte, S., Rankin, A.M., Salmon, R.A., Wolff, E.W., Saiz-Lopez, A., Bloss, W.J., Heard, D.E., Lee, J.D., Plane, J.M.C., 2008. DMS and MSA measurements in the Antarctic Boundary Layer: impact of BrO on MSA production. *Atmos. Chem. Phys.* 8, 2985–2997.
- Saltzman, E.S., Dioumaeva, I., Finley, B.D., 2006. Glacial/interglacial variations in methanesulfonate (MSA) in the Siple Dome ice core, West Antarctica. *Geophys. Res. Lett.* 33, L11811.
- Sievering, H., Cainey, J., Harvey, M., McGregor, J., Nichol, S., Quinn, P., 2004. Aerosol non-sea-salt sulfate in the remote marine boundary layer under clear-sky and normal cloudiness conditions: ocean-derived biogenic alkalinity enhances sea-salt sulfate production by ozone oxidation. *J. Geophys. Res.* 109, D19317.
- Stefels, J., Steinke, M., Turner, S., Malin, G., Belviso, S., 2007. Environmental constraints on the production and removal of the climatically active gas dimethylsulphide (DMS) and implications for ecosystem modelling. *Biogeochemistry* 83, 245–275.
- Sorooshian, A., Lu, M.L., Brechtel, F.J., Jonsson, H., Feingold, G., Flagan, R.C., Seinfeld, J.H., 2007. On the source of organic acid aerosol layers above clouds. *Environ. Sci. Technol.* 41, 4647–4654.
- Savoie, D.L., Prospero, J.M., Larsen, R.J., Saltzman, E.S., 1992. Nitrogen and sulfur species in aerosols at Mawson, Antarctica, and their relationship to natural radio nuclides. *J. Atmos. Chem.* 14, 181–204.
- Savoie, D.L., Prospero, J.M., Larsen, R.J., Huang, F., Izaguirre, M.A., Huang, T., Snowden, T.H., Custals, L., Sanderson, C.G., 1993. Nitrogen and sulfur species in antarctic aerosols at Mawson, Palmer station, and Marsh (King George Island). *J. Atmos. Chem.* 17, 95–122.
- Tao, J., Zhang, Z., Tan, H., Zhang, L., Wud, Y., Sun, J., Chee, H., Cao, J., Cheng, P., Chen, L., Zhang, R., 2018. Observation evidence of cloud processes contributing to daytime elevated nitrate in an urban atmosphere. *Atmos. Environ.* 186, 209–215.
- Tortell, P., Gueguen, C., Long, M., Payne, C., Lee, P., DiTullio, G., 2011. Spatial variability and temporal dynamics of surface water pCO₂, ΔO₂/Ar and dimethylsulfide in the Ross Sea, Antarctica. *Deep Sea Res. Pt. II* 58, 241–259.
- Wang, S., Bailey, D., Lindsay, K., Moore, J.K., Holland, M., 2014. Impact of sea ice on the marine iron cycle and phytoplankton productivity. *Biogeosciences* 11, 4713–4731.
- Von Glasow, R., Crutzen, P.J., 2004. Model study of multiphase DMS oxidation with a focus on halogens. *Atmos. Chem. Phys.* 4 (3), 589–608.
- Wagenbach, D., Ducroz, F., Mulvaney, R., Keck, L., Minikin, A., Legrand, M., Hall, J.S., Wolf, E.W., 1998. Sea-salt aerosol in coastal Antarctic regions. *J. Geophys. Res.* 103, 10961–10974.
- Xu, G., Gao, Y., Lin, Q., Li, W., Chen, L., 2013. Characteristics of water-soluble inorganic and organic ions in aerosols over the Southern Ocean and coastal East Antarctica during austral summer. *J. Geophys. Res. Atmos.* 118, 303–318.
- Yan, J., Lin, Q., Zhao, S., Chen, L., Li, L., 2018. Impact of marine and continental sources on aerosol characteristics using an on-board SPAMS over Southeast Sea, China. *Environ. Sci. Pollution Res.* 25, 30659–30670.
- Yan, J., Jung, J., Zhang, M., Xu, S., Lin, Q., Zhao, S., Chen, L., 2019. Significant underestimation of gaseous methanesulfonic acid (MSA) over Southern Ocean. *Environ. Sci. & Tech.* 53, 13064–13070.
- Young, L.H., Li, C.H., Lin, M.Y., Wang, B.F., Hsu, H.T., Chen, Y.C., Jung, C.R., Chen, K.C., Cheng, D.H., Wang, V.S., Chiang, H.C., Tsai, P.J., 2016. Field performance of semi-continuous monitor for ambient PM_{2.5} water-soluble inorganic ions and gases at a suburban site. *Atmos. Environ.* 144, 376–388.
- Zhang, M., Chen, L., Xu, G., Lin, Q., Liang, M., 2015. Linking phytoplankton activity in polynyas and sulfur aerosols over Zhongshan Station, East Antarctica. *J. Atmos. Sci.* 72, 4629–4642.
- Zhang, M., Gao, W., Yan, J.P., Wu, Y.F., Marandino, C.A., Park, K., Chen, L., Lin, Q., Tan, G., Pang, M., 2019. An integrated sampler for shipboard underway measurement of dimethyl sulfide in surface seawater and air. *Atmos. Environ.* 209, 86–91.
- Zorn, S.R., Drewnick, F., Schott, M., Hoffmann, T., Borrmann, S., 2008. Characterization of the South Atlantic marine boundary layer aerosol using an aerodyne aerosol mass spectrometer. *Atmos. Chem. Phys.* 8, 4711–4728.